IEEE Access
Multidisciplinary ⋮ Rapid Review ⋮ Open Access Journal

Received September 4, 2020, accepted September 14, 2020, date of publication September 18, 2020, date of current version September 30, 2020.

Digital Object Identifier 10.1109/ACCESS.2020.3024691

Hybrid Precoding Technique With Iterative Algorithm for MIMO-OFDM System

SEULGI LEE[1], WON-SEOK LEE[1], JAE-HYUN RO[1], YOUNG-HWAN YOU[2], AND HYOUNG-KYU SONG[1]

[1]Department of Information and Communication Engineering, Sejong University, Seoul 05006, South Korea
[2]Department of Computer Engineering, Sejong University, Seoul 05006, South Korea

Corresponding author: Hyoung-Kyu Song (songhk@sejong.ac.kr)

This work was supported in part by the Ministry of Science and ICT (MSIT) through the Information Technology Research Center (ITRC) Support Program supervised by the Institute for Information and Communications Technology Promotion (IITP), South Korea, under Grant IITP-2019-2018-0-01423, and in part by the Basic Science Research Program through the National Research Foundation of Korea (NRF) funded by the Ministry of Education under Grant 2020R1A6A1A03038540.

ABSTRACT This paper proposes a hybrid precoding technique based on multiple-input multiple-output orthogonal frequency division multiplexing (MIMO-OFDM) system to improve bit error rate (BER) performance in hybrid beamforming system. The conventional hybrid beamforming system cannot outperform the performance of full-digital beamforming system in OFDM. In the proposed algorithm, the analog precoding matrices are designed by iterative algorithm and one proper analog precoding matrix with the highest power of hybrid precoder is selected to achieve the highest performance. According to the number of analog precoding matrices, the diversity gain is increased and the performance is improved. The simulation results show that the BER performance and average sum rate for the proposed scheme are higher than the conventional hybrid beamforming system.

INDEX TERMS Hybrid beamforming, MIMO-OFDM system, analog precoding, iterative algorithms.

I. INTRODUCTION

The beamforming is the representative technique of 5G technology for extensive capacity enhancement. The signal of conventional antennas is radiated evenly in all directions. However, large number of antenna array from transmitter damages the signal due to interference of antenna [1]. Beamforming with multiple input multiple output (MIMO) technology solves such problem. The purpose of transmit beamforming is to maximize the received signal power and increase capacity while the signal to interference plus noise ratio (SINR) is minimized [2], [3]. Capacity improvement is achieved by power control between uplink downlink signals, and enhancement of the signal quality through beamforming. Moreover, beamforming increases the power of downlink signal at the precoding processing because of the coherent combination of the received signals at all antennas [2], [4].

The demand for the increasing wireless data traffic requires massive antennas in 5G communication. A large number of radio frequency (RF) chains for each antenna element increase cost and energy consumption. Therefore, an individual RF chain for each antenna array in full-digital beamforming is infeasible in practical 5G MIMO systems. A promising solution lies in the concept of hybrid transceivers which uses a combination of analog beamformers in the RF domain and digital beamformers in baseband [5]–[8]. Jointly optimized analog and digital beamformers allows hybrid beamformer, to maximize the achievable data [9]. Recent research shows that hybrid beamforming architecture with dynamic antenna subarrays and the hardware-efficient low-resolution phase shifters (PSs) are used in a wideband mmWave MIMO-OFDM system [10].

The existing researches on hybrid precoding in narrowband system to improve the channel capacity have been studied in several ways. The generalized hybrid architecture with a small number of RF chains and a finite number of ADC bits is proposed to achieve the rate performance [11]. The codebook-based hybrid precoding method is adopted in 5G systems with multiple antenna arrays [6], [12], [13]. Additionally, low-resolution hybrid beamforming have been studied recently [14]–[16]. The low-resolution structure has a simple circuit and outputs several parallel signals with different phases. High energy efficiency and low hardware complexity are required by low-resolution structure.

The associate editor coordinating the review of this manuscript and approving it for publication was Zhen Gao.

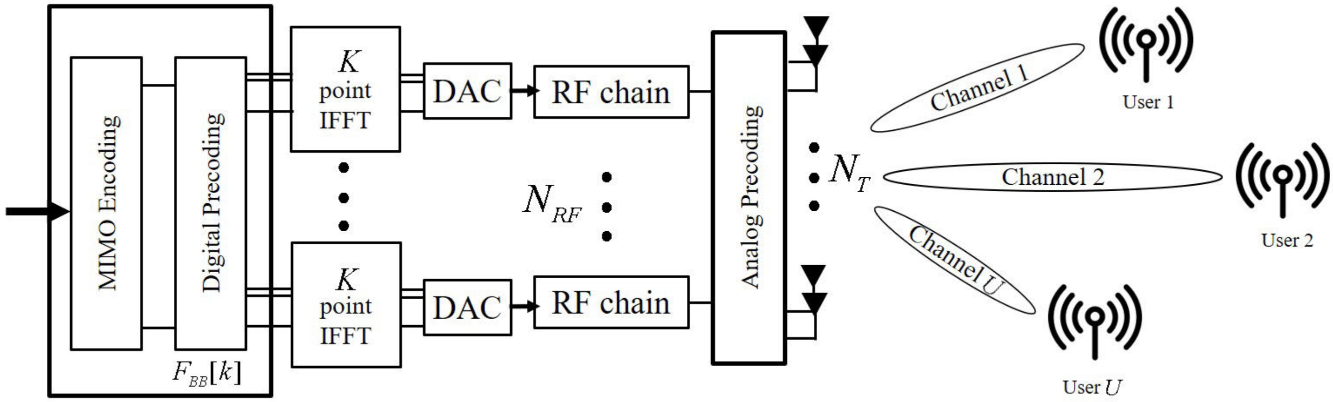

FIGURE 1. Multi-user MIMO-OFDM system based on hybrid beamforming.

On the other hand, several works have been studied in the hybrid beamforming for the wideband OFDM system [18], [19]. In OFDM system, the conventional narrowband hybrid precoding technique is not applicable because each user gets signal through the different subcarrier. The main challenge in designing the hybrid precoding matrix for frequency-selective channel is to select the common analog precoding matrix which adopts at all subcarrier with the digital precoding matrix [17]. In recent research [18], the codebooks were designed with limited channel state information (CSI) based on optimal baseband precoders. Moreover, the joint optimization of wideband analog and digital precoding matrix is necessary to improve performance. Conventional work [19] studied the alternating optimization algorithm of wideband analog precoding matrices and narrowband digital precoding matrices in order to maximize the spectral efficiency. Moreover, the principal component analysis-based broadband hybrid precoder/combiner are designed in the full-connected and sub-connected array [20].

In this paper, the analog precoding matrix is designed by iterative schemes and one proper analog precoding matrix with the highest power of hybrid precoding matrix is selected to achieve the optimal performance of hybrid beamforming in wideband MIMO-OFDM. The main obstacle in hybrid precoding is non-convex problem. Non-convex problem make it difficult to find the hybrid precoding matrix with similar performance of optimal precoding matrix. Hybrid precoding matrix adopts iterative algorithm as the main scheme to solve the non-convex problem [21]–[23].

In iterative process, the digital and analog precoding matrix are updated alternatively by using mean square error (MSE) value between optimal and hybrid precoding matrix in both sub and full connected structures. The proposed algorithm performs analog precoding in each iterative process which finds the precoder with the highest power. This leads to improved performance. Simulation results show that the proposed algorithm with iterative process has higher performance than conventional hybrid beamforming system.

This paper has two main contributions. Firstly, the modified iterative schemes are used in the proposed algorithm in order to accomplish further improvement in spectral efficiency compare to conventional hybrid beamforming algorithm. The existing iterative schemes are used in either sub or full connected structure in narrow band system. However, the modified iterative schemes in the proposed algorithm can be applied on both sub and full connected structure. Further improvement is obtained in wideband MIMO-OFDM system by selecting the best analog precoding matrix among the candidates. The candidates are determined by the modified iterative scheme in all points of FFT.

Secondly, the proposed algorithm improves the performance of BER and spectral efficiency of conventional hybrid beamforming system in order to approach full-digital beamforming system with the limited number of antennas. Large antenna arrays are essential to get enough performance of hybrid beamforming system. However, high cost and power consumption constrain the usage of large number of antenna in hardware hybrid beamforming system. In this proposed paper, the same number of antenna array is used in both full-digital and hybrid beamforming system in order to demonstrate the improvement of the performance.

II. HYBRID BEAMFORMING SYSTEM MODEL FOR MIMO-OFDM

Fig. 1 shows a wireless multi-user MIMO-OFDM system with N_T transmit antennas and U user devices [7], [24]. The data streams are demodulated into sub-streams in encoder and each substream is mapped to the phase shift keying (PSK) or quadrature amplitude modulation (QAM) symbol. OFDM symbols with K sub-carriers are proceeded by inverse fast Fourier transform (IFFT) and combined with cyclic prefix (CP) before precoding in RF chain. In the analog precoding, the precoding matrix can be implemented by phase shifters with variable gain amplifiers. In this section, two kinds of hybrid beamforming structures, tranceiver structure and channel model are described.

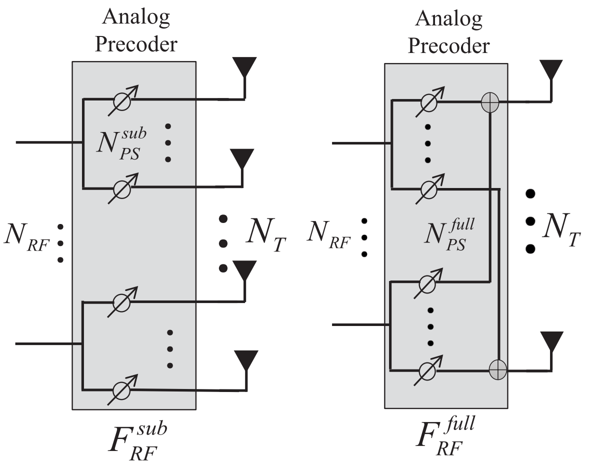

(a) Sub-connected structure (b) Full-connected structure

FIGURE 2. Two kinds of hybrid beamforming structures.

A. STRUCTURE OF HYBRID BEAMFORMING SYSTEM

Fig. 2 shows two structures of analog precoder in hybrid beamforming system according to the connection method of phase shifters. In the sub-connected structure, each phase shifter is connected to each antenna array. On the other hand, in the full-connected structure, each phase shifter of RF chains is connected to one of antenna arrays. The full-connected structure has higher hardware complexity and performance than sub-connected structure.

The RF chains and phase shifters are used in multi-user MIMO system with N_T antenna array. The number of RF chains N_{RF} and data streams N_s is same, i.e. $N_{RF} = N_s$. The matrix of digital precoding in the k-th subcarrier, $\mathbf{F}_{BB}[k]$, has the same size in two structures with $\mathbf{F}_{BB}[k] \in \mathbb{C}^{N_{RF} \times N_s}$, $k = 1, 2, \cdots, K$. Analog precoding matrix $\mathbf{F}_{RF} \in \mathbb{C}^{N_T \times N_{RF}}$ has the unit modulus norm on all elements. The matrix of analog precoding has two different shapes according to structure of hybrid beamforming system. Analog precoding matrix in sub-connected structure is as follows,

$$\mathbf{F}_{RF}^{sub} = \begin{bmatrix} \mathbf{f}_1^{sub} & 0 & \cdots & 0 \\ 0 & \mathbf{f}_2^{sub} & \cdots & 0 \\ \vdots & \vdots & \ddots & \vdots \\ 0 & 0 & \cdots & \mathbf{f}_{N_{RF}}^{sub} \end{bmatrix}, \quad (1)$$

where $\mathbf{f}_n^{sub}$ is the n-th column vector, $n = 1, 2, \cdots, N_{RF}$ with size of $N_{PS}^{sub} \times 1$. N_{PS}^{sub} is the number of phase shifter (PS) which is connected to one RF chain.

The number of phase shifters, N_{PS}^{full}, and total antennas N_T is same since each phase shifter in all RF chains is connected to one of antenna arrays in full-connected structure. Analog precoding matrix in full-connected structure is as follows,

$$\mathbf{F}_{RF}^{full} = \begin{bmatrix} \mathbf{f}_1^{full} & \mathbf{f}_2^{full} & \cdots & \mathbf{f}_{N_{RF}}^{full} \end{bmatrix}, \quad (2)$$

where $\mathbf{f}_n^{full}$ is the n-th column vector, $n = 1, 2, \cdots, N_{RF}$ with size of $N_T \times 1$.

B. SIGNAL MODEL IN HYBRID BEAMFORMING

In the multi-user OFDM-MIMO based on hybrid beamforming system, the digital precoding matrix at the k-th subcarrier, $\mathbf{F}_{BB_u}[k]$, exists for all subcarriers. The digital precoding matrix transforms the signals to the time domain by using K-points IFFT. Since the analog precoder is a post-IFFT module, the analog precoding matrix is identical for all subcarriers. Therefore, the final transmitted signal at subcarrier k is as follows,

$$\mathbf{x}[k] = \sum_{u=1}^{U} \mathbf{F}_{RF}\mathbf{F}_{BB_u}[k]\,\mathbf{s}_u[k], \quad (3)$$

where $\mathbf{s}_u[k] \in \mathbb{C}^{N_s \times 1}$ is the vector of the data stream at each subcarrier $k = 1, 2, \cdots, K$ in the u-th user. All devices have N_r antennas. The channel matrix is $\mathbf{H}[k] \in \mathbb{C}^{N_r \times N_T}$. The received signal in the u-th user can be expressed as follows [6],

$$\mathbf{y}_u[k] = \mathbf{H}_u[k]\mathbf{F}_{RF}\mathbf{F}_{BB_u}[k]\mathbf{s}_u[k] + \mathbf{H}_u[k]\sum_{i \neq u}^{U} \mathbf{F}_{RF}\mathbf{F}_{BB_i}[k]\mathbf{s}_i[k] + \mathbf{n}_u[k], \quad (4)$$

where $\mathbf{n}_u[k]$ represents the additive white Gaussian noise(AWGN) vector of the u-th user. The combiner is performed by phase shifters and expressed by $\left|\mathbf{W}_{RF_u}(i,j)\right| = 1, \forall (i,j)$ where the all elements of matrix are the unit modulus norm. $\mathbf{W}_{RF_u}$ down-converts the signals to the baseband with RF chains in user device. Therefore, devices use a low-dimensional digital combiner,$\mathbf{W}_{BB_u}$, and the final processed signals are obtained as follows,

$$\tilde{y}_u[k] = \mathbf{W}_u[k]\mathbf{H}_u[k]\mathbf{F}_u[k]\mathbf{s}_u[k] + \mathbf{W}_u[k]\mathbf{H}_u[k]\sum_{i \neq u}^{U} \mathbf{F}_i[k]\mathbf{s}_i[k] + \tilde{\mathbf{W}}, \quad (5)$$

where $\mathbf{W}_u[k] = \mathbf{W}_{RF_u}\mathbf{W}_{BB_u}[k]$ and $\mathbf{F}_u[k] = \mathbf{F}_{RF}\mathbf{F}_{BB_u}[k]$. $\tilde{\mathbf{W}}$ is the noise vector with combiner matrix. And $R_u[k]$ is the spectral efficiency of the k-th subcarrier as follows [6],

$$R_u[k] = \log_2 \left| \mathbf{I}_{N_s} + \mathbf{W}_u[k]\mathbf{C}_u^{-1}[k]\mathbf{W}_u{}^H[k] \times \mathbf{H}_u[k]\mathbf{F}_u[k]\mathbf{F}_u^H[k]\mathbf{H}_u^H[k] \right|, \quad (6)$$

where $\mathbf{C}_u[k]$ is the covariance of the interference plus noise at the u-th user. $\mathbf{I}_{N_s}$ is the identity matrix with size of N_s.

C. CHANNEL MODEL

The beamforming system uses 3D channel model [25] with zenith and azimuth angle on geometric stochastic model to determine accurate beamforming precoder. Although, the perfect channel information cannot be acquired, the perfect channel information is assumed to show the maximum performance of the proposed algorithm. If the specific technique for the channel estimation is used, the performance can be degradation. The multi-user channel model is composed of single-user channels as follows,

$$\mathbf{H} = \begin{bmatrix} \mathbf{H}_1 \\ \vdots \\ \mathbf{H}_u \\ \vdots \\ \mathbf{H}_U \end{bmatrix} \tag{7}$$

The u-th users 3D channel is suggested by the Saleh-Valenzuela model [6] as follows,

$$\mathbf{H}_u = \sqrt{\frac{N_t N_r}{L}} \sum_{l=1}^{L} \alpha_{l,u} \mathbf{a}_{r,u}\left(\phi_{l,u}^r, \theta_{l,u}^r\right) \mathbf{a}_{t,u}\left(\phi_{l,u}^t, \theta_{l,u}^t\right)^H, \tag{8}$$

where $\alpha_{l,u}$ denotes the complex gain of the l-path. In addition, $\mathbf{a}_{r,u}\left(\phi_{l,u}^r, \theta_{l,u}^r\right)$ and $\mathbf{a}_{t,u}\left(\phi_{l,u}^t, \theta_{l,u}^t\right)$ represent the transmit and receive array response vector, where $\phi_{l,u}^r$ and $\phi_{l,u}^t$ stand for the azimuth angle of arrival (AoA) and departure (AoD) $\theta_{l,u}^r, \theta_{l,u}^t$ are the zenith of AoA and AoD. In this paper, antenna array considers the uniform planar array (UPA) in one plane with W and H elements on the each axes and the array response vector is given by [6], [26],

$$\mathbf{a}_{UPA}(\phi, \theta) = \frac{1}{\sqrt{N_{Tx}}}\left[e^{j\varphi(0,0)}, \cdots, e^{j\varphi(m,n)}, \cdots, e^{j\varphi(W-1,H-1)}\right]^T, \tag{9}$$

where $0 \leq m < W$ and $0 \leq n < H$ are the number of antenna elements in each axis and $\varphi(m,n) = kd(m \sin\phi \sin\theta) + n\cos\theta$. The total number of antenna arrays is $N = WH$. Also, k and d are the antenna spacing and the signal wave length.

III. THE CONVENTIONAL HYBRID PRECODING METHOD IN MIMO-OFDM

This section explains conventional hybrid beamforming in MIMO-OFDM with analog and digital precoding. Both precoding matrices are used together as hybrid precoder. Analog precoding matrix is determined by antenna array and digital precoding matrix. The digital precoding matrix is designed by MIMO detection algorithm with effective channel [27], [28].

The analog precoding matrix regard the location matrix of antenna array $\mathbf{A}$ which have three columns to express 3D antenna array with rectangular coordinate system. Each column of matrix $\mathbf{A}$ is about the antenna in each axis. In this paper, the first column vector of the matrix $\mathbf{A}$ is all zeros since UPA antenna array uses only two axises. The location matrix of antenna array $\mathbf{A}$ is given as follows,

$$\mathbf{A} = \begin{bmatrix} \mathbf{A}_0 \\ \mathbf{A}_1 \\ \vdots \\ \mathbf{A}_n \end{bmatrix}, \quad n = 0, 1, \cdots, N_y - 1, \tag{10}$$

where the size of matrix, A_n, is $N_z \times 3$. N_y, N_z are the number of antennas on each axis. (10) expresses the matrix $\mathbf{A}$ divided by N_y and the $\mathbf{A}_n$ should instruct about N_z. A_n is expressed as follows,

$$\mathbf{A}_n = \begin{bmatrix} 0 & n & 0 \\ 0 & n & 1 \\ \vdots & \vdots & \vdots \\ 0 & n & N_z - 1 \end{bmatrix}. \tag{11}$$

Because the sub-connected structure has N_{RF} antenna arrays with N_{PS}^{sub} phase shifters in each RF chain, the location matrix of antenna array is $\mathbf{A} \in \mathbb{Q}^{N_{PS}^{sub} \times 3}$. On the other hand, because all transmit antennas consists of the one array, the location vector matrix of antenna array is $\mathbf{a} \in \mathbb{Q}^{N_T \times 3}$.

The azimuth (ϕ) and zenith (θ) are decided by the n-th RF chain antenna array is used to make analog precoding matrix [29]. The antenna array in the n-th RF chain of direction vector in Cartesian coordinates is as follows [25],

$$\mathbf{r}_n = \begin{bmatrix} \sin\theta\cos\phi \\ \sin\theta\sin\phi \\ \cos\phi \end{bmatrix}. \tag{12}$$

Finally, the column vector element of the analog precoding matrix is expressed with vector $\mathbf{f}_n = \mathbf{A}\mathbf{r}_n$as follows,

$$\begin{aligned} \mathbf{f}_n^{sub} &= \left[e^{j\angle \mathbf{f}_n(1)} \quad e^{j\angle \mathbf{f}_n(2)} \quad \cdots \quad e^{j\angle \mathbf{f}_n(N_{PS}^{sub})}\right]^T, \\ \mathbf{f}_n^{full} &= \left[e^{j\angle \mathbf{f}_n(1)} \quad e^{j\angle \mathbf{f}_n(2)} \quad \cdots \quad e^{j\angle \mathbf{f}_n(N_T)}\right]^T \end{aligned} \tag{13}$$

where each vector denotes the n-th column vector of the analog precoder matrix $\mathbf{F}_{RF}$ in sub-connected and full-connected structure.

The digital precoding matrix is determined by the analog precoding matrix and effective channel matrix. Because the channel matrix contains the analog beamforming effect, the effective channel is used to make digital precoding matrix. The effective channel is expressed as follows,

$$\mathbf{H}_e[k] = \mathbf{H}[k]\mathbf{F}_{RF}, \quad k = 1, 2, \cdots, K, \tag{14}$$

where the k is the sub-carrier order. In this paper, the digital precoding matrix, $\mathbf{F}_{BB}$, is also fixed by effective channel with zero forcing (ZF) method. The conventional hybrid beamforming system has lower hardware cost and complexity than full-digital beamforming system which is infeasible in practical 5G systems. More precisely, when the number of antennas is usually very large, the hybrid performance can approach the full-digital beamforming [5]. When the same number of antennas is used in both hybrid and full-digital beamforming system, the hybrid beamforming performance cannot approach the full-digital performance. In this paper, the proposed hybrid beamforming system approach the performance of the full-digital beamforming with the same number of antennas in wideband MIMO-OFDM.

IV. THE PROPOSED HYBRID PRECODING WITH ITERATIVE ALGORITHM

The proposed hybrid precoding technique uses the modified iterative algorithm to cope with the non-convex problem and defines the analog precoding matrix that improves the performance. The three iterative algorithms [21]–[23] are used in sub-connected and full-connected structures of hybrid beamforming system. The algorithm uses iterative schemes in all K points of subcarriers to make candidates of analog precoding matrix. One common analog precoding matrix with the best performance is selected among the candidates. In modified iterative scheme, the optimal precoding matrix, $\mathbf{F}_{opt}$, is necessary to start iterative algorithm. $\mathbf{F}_{opt}$ is calculated by full-digital beamforming system which provides the optimal performance in beamforming. Thus, the hybrid precoding matrix should consider the non-convex problem with objective function as follows,

$$\begin{aligned} &\underset{\mathbf{F}_{RF},\mathbf{F}_{BB}}{\arg\min} \ \left\|\mathbf{F}_{RF}\mathbf{F}_{BB}-\mathbf{F}_{opt}\right\|_F^2 \\ &\text{Subject to. } |\mathbf{F}_{RF}\,(i,j)| = 1 \ \ (\forall i,j) \\ &\qquad\qquad \|\mathbf{F}_{RF}\mathbf{F}_{BB}\|_F^2 = N_s. \end{aligned} \tag{15}$$

In the hybrid precoding scheme, the precoding matrix can be expressed as digital precoding matrix, $\mathbf{F}_{BB}$, and RF analog precoding matrix, $\mathbf{F}_{RF}$ such that $\mathbf{F}_{opt} = \mathbf{F}_{RF}\mathbf{F}_{BB}$. However, the differentiation cannot be used to determine hybrid precoding matrix because $\mathbf{F}_{RF}$ has fixed amplitude and $\mathbf{F}_{BB}$ has fluctuated phase and amplitude. Due to such issue, the iterative scheme is used to get the values of $\mathbf{F}_{RF}$ and $\mathbf{F}_{BB}$.

In the proposed algorithm, the iterative schemes [21]–[23] are used in OFDM system and modified to apply both sub-connected and full-connected structure. The optimal precoding matrix and the initialized analog precoding matrix $\mathbf{F}_{RF}^{(0)}$ are the common input values in the three iterative algorithms. The optimal precoding matrix is determined by full digital beamforming scheme and the initialized analog precoding matrix is suggested by (13).

The modified Alternating, Langrange Multiplier, PE-AltMin methods update the initialized analog precoder in different ways to set the final analog precoding matrix. The modified Alternating algorithm is the hybrid precoding algorithm which is developed to optimize the analog and digital beamforming matrices. The algorithm modifies the size of used optimal precoder matrix $\mathbf{F}_{opt}$ in order to apply on full-connected structure. The analog and digital precoding matrix are updated to maximize the sum rate with different practical constraints. The elements of analog precoding matrix in sub-connected and full-connected structure are updated as follows,

$$\begin{aligned} \mathbf{f}_n^{sub} &= \mathbf{F}_{opt}^n \mathbf{f}_{BB}^{n\ H} \\ \mathbf{f}_n^{full} &= \mathbf{F}_{opt} \mathbf{f}_{BB}^{n\ H}, \end{aligned} \tag{16}$$

where $\mathbf{F}_{opt}^n$ denotes the n-th block matrix of $\mathbf{F}_{opt}$ with size of $N_{PS}^{sub} \times 1$ and $\mathbf{f}_{BB}^n$ is the n-th row vector of digital precoding matrix $\mathbf{F}_{BB}$. The $\mathbf{F}_{opt}$ is as follows,

$$\mathbf{F}_{opt} = \begin{bmatrix} \mathbf{F}_{opt}^1 & & \cdots & \\ & \mathbf{F}_{opt}^2 & & \vdots \\ \vdots & & \ddots & \\ & \cdots & & \mathbf{F}_{opt}^n \end{bmatrix}. \tag{17}$$

One iterative process is completed when the all row vectors of matrix are updated by (16).

The modified Langrange Multiplier uses the block matrix of $\mathbf{G} = \mathbf{F}_{opt} - \sum_{i=1,i\neq n}^{N_{RF}} \mathbf{f}_{RF}^i \mathbf{f}_{BB}^i$ to make sub-connected structure of analog precoding matrix. $\mathbf{f}_{RF}^i$ is the i-th column vector of analog precoding matrix $\mathbf{F}_{RF}$. The modified method updates only one column of the analog precoding matrix affected by one row of the digital precoding matrix. Each element of sub-connected and full-connected structure of analog precoding matrix is updated as follows,

$$\begin{aligned} \mathbf{f}_n^{sub} &= \mathbf{G}_n \mathbf{f}_{BB}^{n\ H} \\ \mathbf{f}_n^{full} &= \mathbf{G} \mathbf{f}_{BB}^{n\ H}, \end{aligned} \tag{18}$$

where $\mathbf{G}_n$ is the n-th block matrix of $\mathbf{G}$ with size of $N_{PS}^{sub} \times 1$ as $\mathbf{F}_{opt}$. The one iteration is completed by updating all elements of analog precoder. The modified Lagrange Multiplier iterative scheme has high performance when the number of RF chains is more than twice the number of data stream.

The modified PE-AltMin method uses block matrix of optimal precoding matrix in order to update both sub-connected and full-connected analog precoding matrix. The singular value decomposition (SVD) method is used to update precoding matrix. The complexity of PE-AltMin is lower than Alternating and Langrange Multiplier method. The updated elements of analog precoding matrix are given as follows,

$$\begin{aligned} \mathbf{f}_n^{sub} &= \mathbf{F}_{opt}^n \mathbf{t}_n^{\ H} \\ \mathbf{f}_n^{full} &= \mathbf{F}_{opt} \mathbf{t}_n^{\ H}, \end{aligned} \tag{19}$$

where $\mathbf{t}_n$ is the n-th row vector of $\mathbf{T} = \mathbf{V}_1\mathbf{U}^H$ which comes from the SVD of $\mathbf{F}_{opt}^H\mathbf{F}_{RF} = \mathbf{U}\Sigma\mathbf{V}_1{}^H$. Σ is a diagonal matrix and U, $\mathbf{V}_1$ are the unitary matrices.

When the analog precoding matrix is updated by iterative algorithm, the digital precoding matrix is also fixed by ZF method that uses effective channel as illustrated in (14). The analog and digital precoding matrices are repeatedly updated until the gap between prior $(i-1)$-th MSE value δ_{i-1} and the i-th MSE value δ_i is smaller than the threshold τ. The i-th MSE value δ_i is as follows,

$$\delta_i = \left\|\mathbf{F}_{opt} - \mathbf{F}_{RF}^{(i)}\mathbf{F}_{BB}\right\|_F^2. \tag{20}$$

where the optimal precoding matrix, $\mathbf{F}_{opt}$, is calculated by full digital beamforming scheme. The number of iteration is determined by residual value δ. After iterative algorithm updates the analog and digital precoding matrices, $\mathbf{F}_{RF}$, $\mathbf{F}_{BB}$, the i-th MSE value δ_i is calculated to find the gap between prior $(i-1)$-th MSE value δ_{i-1} until the gap is smaller than threshold τ. A detailed description of the iterative scheme at the k-th subcarrier is shown in Algorithm 1.

The iterative scheme is used to make analog precoding matrix with equivalent number of subcarriers. As a result, according to the number of subcarriers, the analog precoding matrix $\mathbf{F}_{RF}^{(i)}$ is designed as set $\mathbf{\Theta}_{RF}$ demonstrated as follows,

$$\mathbf{\Theta}_{RF} = \left\{\mathbf{F}_{RF,1}, \mathbf{F}_{RF,2}, \cdots, \mathbf{F}_{RF,K}\right\}. \tag{21}$$

Algorithm 1 Iterative Algorithm at the k-th Subcarrier

Data: CSI of $\mathbf{H}[k]$, $\mathbf{F}_{opt}[k]$

Result: $\mathbf{F}_{RF}^{(0)}$

(1) initialize $i = 0,\ \delta_0 = 0$, $\mathbf{F}_{RF}^{(0)}$ by (12)

(2) **while** $\delta_i - \delta_{i-1} < \tau$

(3) **do** find $\mathbf{F}_{RF}^{(i)}$

(4) $\mathbf{H}_e[k] = \mathbf{H}[k]\mathbf{F}_{RF}^{(i)}$

(5) $\mathbf{F}_{RF}^{(i)}[k] = \left(\mathbf{H}_e^H[k]\mathbf{H}_e[k]\right)^{-1}\mathbf{H}_e^H[k]$

(6) Compute the SVD: $\mathbf{F}_{opt}^H\mathbf{F}_{RF}^{(i)} = \mathbf{U}\Sigma\mathbf{V}_1^H$, $\mathbf{T} = \mathbf{V}_1\mathbf{U}^H$

(7) **for** $n = 1, 2, \cdots, N_{RF}$

(8) $\mathbf{G} = \mathbf{F}_{opt} - \sum_{k=1,k\neq n}^{N_{RF}} \mathbf{f}_{RF}^{k(i)}\mathbf{f}_{BB}^{k}$

(9) Alternating Method: $\mathbf{f}_n^{sub} = \mathbf{F}_{opt}^n \times (\mathbf{f}_{BB}^n)^H$ or $\mathbf{f}_n^{full(i+1)} = \mathbf{F}_{opt}(\mathbf{f}_{BB}^n)^H$

Langrange Multiplier Method: $\mathbf{f}_n^{sub(i+1)} = \mathbf{G}_n \times (\mathbf{f}_{BB}^n)^H$ or $\mathbf{f}_n^{full(i+1)} = \mathbf{G} \times (\mathbf{f}_{BB}^n)^H$

PE-AltMin Method: $\mathbf{f}_n^{sub(i+1)} = \mathbf{F}_{opt}^n \times (\mathbf{t}_n)^H$ or $\mathbf{f}_n^{all(i+1)} = \mathbf{F}_{opt} \times (\mathbf{t}_n)^H$

(10) **end**

(11) $i = i + 1$

(12) $\delta_i = \left\|\mathbf{F}_{opt}[k] - \mathbf{F}_{RF}^{(i)}\mathbf{F}_{BB}^{(i)}[k]\right\|_F^2$

(13) **end** $\mathbf{F}_{RF}^{(i)}$

The element of set $\mathbf{F}_{RF,s} \in \mathbf{\Theta}_{RF}$ is the result of iterative scheme $\mathbf{F}_{RF}^{(i)}$ at the s-th point of subcarrier. The performance is further improved compare to conventional hybrid algorithm since the set of analog precoding matrix gives diversity gain. The analog precoding matrix should be selected since each data stream is modulated by one analog beamformer in hybrid beamforming system.

Before one analog precoding matrix is selected, the digital precoding matrix $\mathbf{F}_{BB}$ should be calculated by effective channel. The effective channel is given as follows,

$$\mathbf{H}_e[k] = \mathbf{H}[k]\mathbf{F}_{RF,s}. \tag{22}$$

The digital precoding matrix is calculated as follows,

$$\mathbf{F}_{BB}[k] = \left(\mathbf{H}_e^H[k]\mathbf{H}_e[k]\right)^{-1}\mathbf{H}_e^H[k]. \tag{23}$$

Hence, hybrid precoding matrix is formed as the same number of subcarriers. The digital precoding matrix $\mathbf{F}_{BB}$ has different norm according to analog precoding matrix, so the different norm of hybrid precoding matrix is existed. The one hybrid precoding matrix with the smallest norm is selected as follows,

$$(\mathbf{F}_{RF}, \mathbf{F}_{BB}) = \underset{(\mathbf{F}_{RF,s}, \mathbf{F}_{BB})}{\arg\min} \sum_{k=1}^{K} \left\|\mathbf{F}_{RF,s}\mathbf{F}_{BB}[k]\right\|_F^2. \tag{24}$$

The selected precoding matrix is the best precoder which provides the best performance among the candidates. The Fig. 3 is a flow chart of proposed algorithm with iterative precoding scheme in hybrid beamforming system. According to the number of analog precoding matrix, the diversity gain is increased. Iterative process in all K subcarriers has the maximum complexity and the highest performance of proposed precoding scheme. With some sacrifice of performance, the complexity of operation can be reduced by decreasing the number of subcarriers. In addition to the iterative algorithm, the proposed scheme can improve performance by obtaining a diversity gain in OFDM system no matter what hybrid precoding scheme is used in each point of subcarrier.

In order to know the selective probability expectation, the Fig. 4 shows the normalized histogram with the probability density function (pdf). In Fig. 4, the normalized histogram is about the inverse values of precoding matrix γ_s in the iteration results of full-connected PE-AltMin method. The γ_s is as follows,

$$\gamma_s = \left(\sum_{k=1}^{K} \left\|\mathbf{F}_{RF,s}\mathbf{F}_{BB}[k]\right\|_F^2\right)^{-1}. \tag{25}$$

The pdf of histogram is shown as the Lognormal distribution $p(\gamma_s)$. If the γ is the largest value of γ_s, the pdf of selecting the largest norm is shown as follows,

$$p(\gamma_s < \gamma) = \Phi\left(\frac{\ln\gamma - \mu}{\sigma}\right), \tag{26}$$

where the Φ is the cumulative distribution function (cdf) of normal distribution $N(\mu, \sigma^2)$. Since the γ_s are independent,

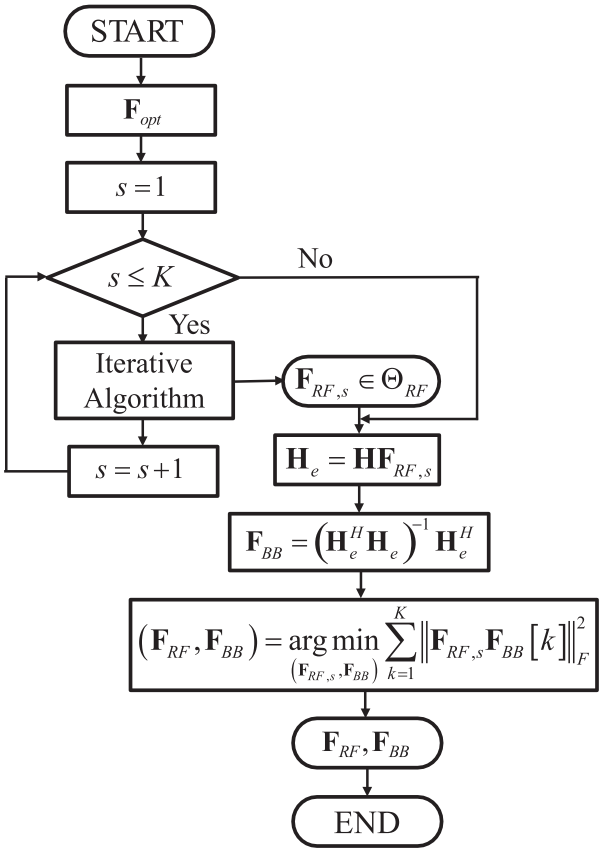

FIGURE 3. The flow chart of proposed precoding algorithm.

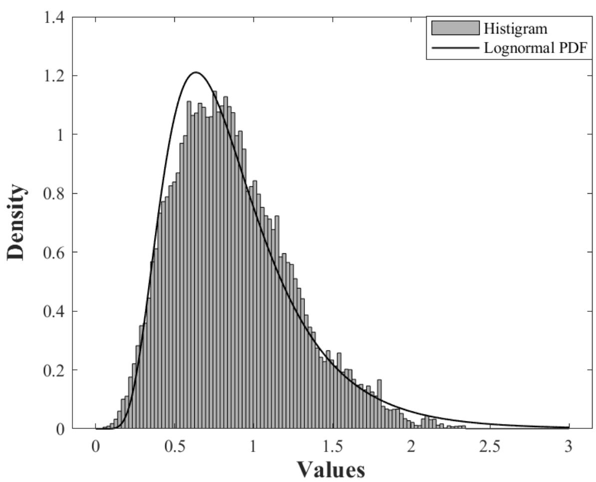

FIGURE 4. The normalized histogram and Lognormal distribution pdf.

the probability can be expressed simply. The distribution cdf of γ in the number of the picked FFT points p is shown as follows [30],

$$G_p(\gamma) = \left(\Phi\left(\frac{\ln\gamma - \mu}{\sigma}\right)\right)^p. \tag{27}$$

The expectation of $G_p(\gamma)$ as follows as,

$$\bar{\gamma}(p) = \int_0^\infty \gamma \, dG_p(\gamma). \tag{28}$$

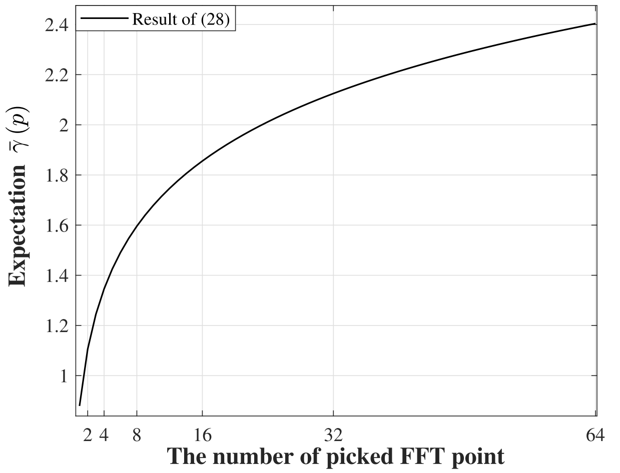

FIGURE 5. The expectation according to the number of picked FFT point.

When the iteration method is used in the p picked FFT points, the gain is obtained by the expectation as $\bar{\gamma}(p)$. The result of (28) is shown as Fig. 5. It is clear that the increased number of picked FFT point gives high diversity gain and the gain is gradually decreased. Based on numerical results of the proposed algorithm, graphical results are shown in Section V.

V. SIMULATION RESULTS

For evaluating the performance of the proposed algorithm, BER performances, average sum rate and computational complexity are measured. The simulations in this paper are performed on the MIMO-OFDM system with sub-connected and full-connected structure of hybrid beamforming system. The simulation parameters in TABLE 1 are used. The antenna array in (9) is separated by a half wavelength distance with $W = N_T$ and $H = 1$. There are several channel estimation methods in hybrid beamforming system [31], [32]. However, in simulation results, the perfect channel estimation is assumed to show the performances of proposed algorithm. The minimum number of RF chain to receive the transmit signals in both sub and full connected structures has the same number of data streams. The conventional hybrid beamforming algorithm is used as Section III with the same antenna array. The beam steering method [29] is applied on designing analog precoding matrix. The iterative algorithm is not used to design the analog precoding matrix. According to the θ and ϕ of $\mathbf{r}_n$ which is determined by the channel information and the antenna array matrix $\mathbf{A}_n$, the analog precoding matrix is set up. The effective channel can be calculated as (14). ZF method is combined with effective channel to design the digital precoding matrix. Number of antenna and RF chain used are same as TABLE 1 in each structure.

Fig. 6 and Fig. 7 show the results of each iterative algorithm which is used in all 64 points of subcarriers to make analog precoding matrices. Fig. 6 compares the proposed algorithm with conventional hybrid beamforming system in sub-connected structure. The conventional beamforming

TABLE 1. Simulation parameters.

	Sub-connected structure	Full-connected structure
Number of data streams	4	2
Number of RF chains	4	2
Number of transmit antennas	16	8
Number of user devices	4	2
Number of antenna in each device	1	
Number of subcarriers	64	
CP size	16	
Modulation Order	QPSK	
Number of multi-path	7	

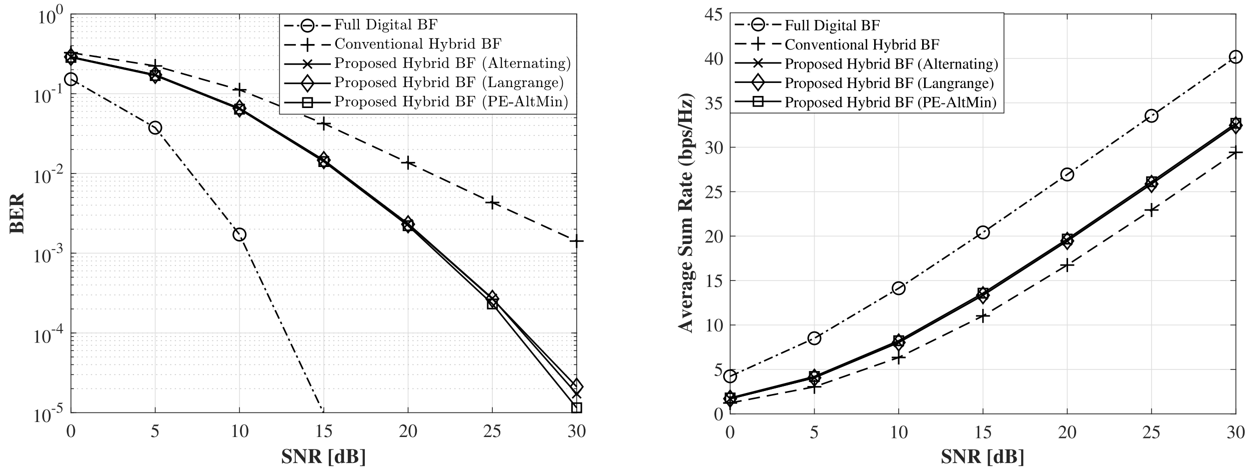

(a) The BER performance (b) The average sum rate performance

FIGURE 6. The performances of proposed and conventional algorithms in sub-connected structure with each iterative scheme at all 64 points.

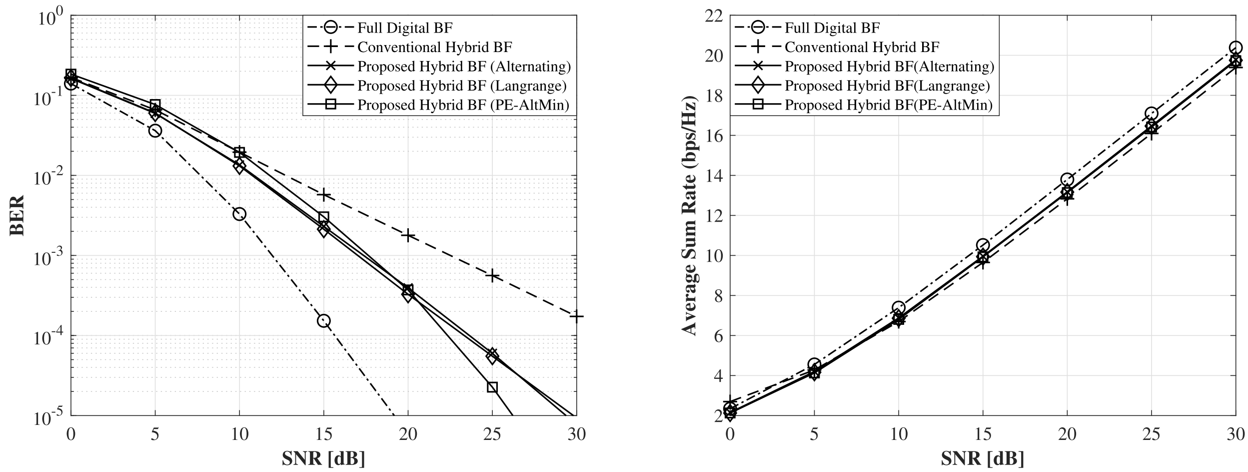

(a) The BER performance (b) The average sum rate performance

FIGURE 7. The performances of proposed and conventional algorithms in full-connected structure with each iterative scheme at all 64 points.

system has lower performance than the proposed system in both BER and average sum rate. This is because the analog precoding matrix and digital precoding matrix are not jointly optimized to improve the performance. According to the number of analog precoding matrix, the diversity gain is obtained to improve the performance.

The full digital beamforming system operates on the same number of transmit antennas and data streams which has the optimal performance. Fig. 6a shows the BER performance of proposed and conventional algorithms in sub-connected structure with three different iterative schemes at all 64 points of subcarriers. Three iterative schemes i.e. modified

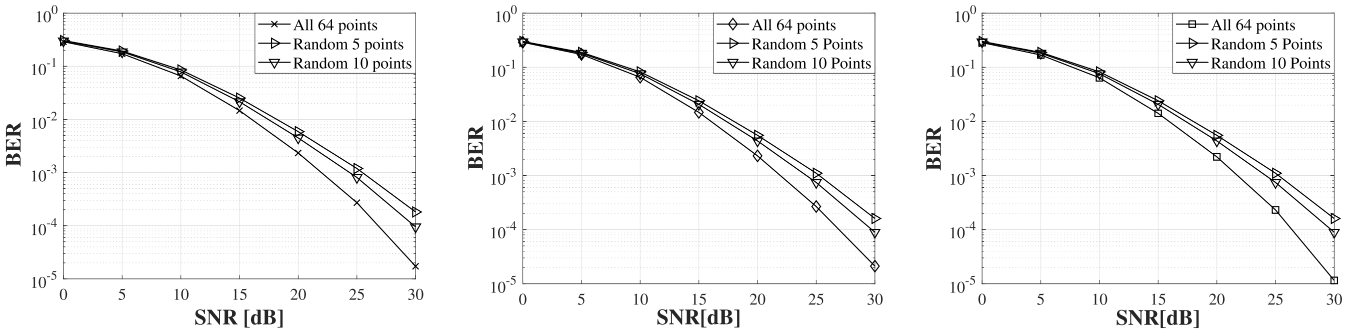

(a) The modified Alternating method (b) The modified Langrange Multiplier method (c) The modified PE-AltMin method

FIGURE 8. **The three BER performances of each modified iterative methods in sub-connected structure according to the different number of subcarriers.**

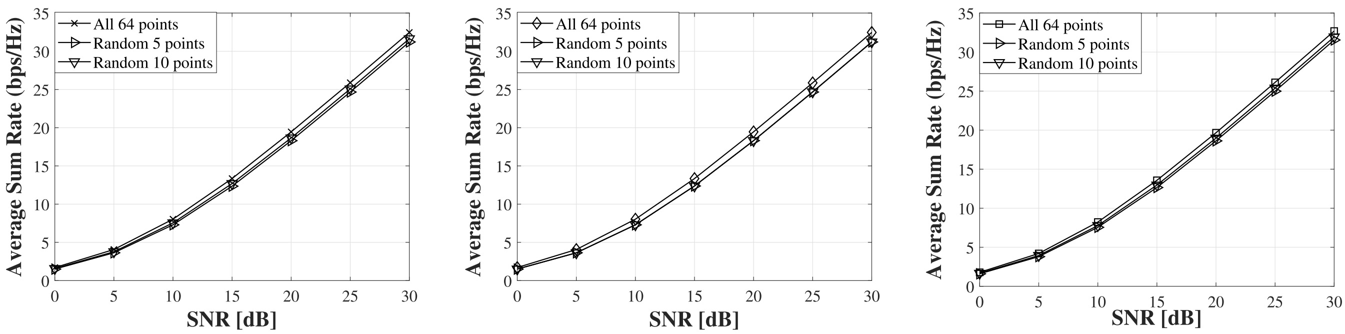

(a) The modified Alternating method (b) The modified Langrange Multiplier method (c) The modified PE-AltMin method

FIGURE 9. **The three average sum rate performances of each modified iterative methods in sub-connected structure according to the different number of subcarriers.**

Alternating, modified Langrange Multiplier and modified PE-AltMin are used in the proposed algorithm which are the representative methods for hybrid beamforming precoding. The proposed algorithm with iterative scheme finds the smallest MSE value δ between $\mathbf{F}_{opt}$ and hybrid precoding matrix. Also, the proposed algorithm has better performance than the conventional system since the diversity gain is obtained.

Fig. 6b shows the average sum rate of proposed and conventional algorithm in sub-connected structure with each iterative scheme at all 64 points of subcarriers. In this paper, the zero-mean and unit variance AWGN and 3D channel model are used. The sum rate of the u-th user C_u is given as follows,

$$C_u = \sum_{k=1}^{K} \log_2 \left(1 + \left\|\mathbf{H}[k]\mathbf{F}_{RF}\mathbf{F}_{BB_u}[k]\mathbf{s}_u[k]\right\|_F^2\right). \quad (29)$$

The proposed algorithm with iterative schemes at all 64 points have higher average sum rate than conventional algorithm. The performance improvement at the all SNR is 3bps/Hz gain compared to the conventional scheme.

Fig. 7 shows the BER and average sum rate of the proposed and conventional algorithms in full-connected structure. Fig. 7a compares the BER performance of the proposed and conventional algorithms in full-connected structure with each iterative scheme at all 64 points of subcarriers. The modified PE-AltMin method has the best performance among three iterative algorithms because the modified PE-AltMin method is optimized at the full-connected structure.

Fig. 7b shows the average sum rate of the proposed and conventional algorithms in full-connected structure with each iterative scheme at all 64 points of subcarriers. The full-connected structure performance has more closer to full digital beamforming system than sub-connected structure because full-connected structure has more accurate analog precoding matrix than sub-connected structure. In this paper, the number of analog precoding matrix gives the diversity gain to improve the performance. The proposed algorithm requires iteration process to make analog and digital precoding matrix at all of subcarriers However, the complexity of proposed algorithm is high and it has the best performance. For decreasing complexity, the proposed algorithm randomly picks 5 and 10 points of subcarriers to make the small number of analog precoding matrix.

Fig. 8 show the BER performance and Fig. 9 show the average sum-rate of three iterative schemes, i.e. Alternating, Langrange Multiplier and PE-AltMin respectively to make analog precoding matrix at 5, 10 and all subcarriers in sub-connected structure.

Fig. 10 also show the BER performance of three iterative schemes in full-connected structure. In the proposed algorithm, performance increases as the number of used points

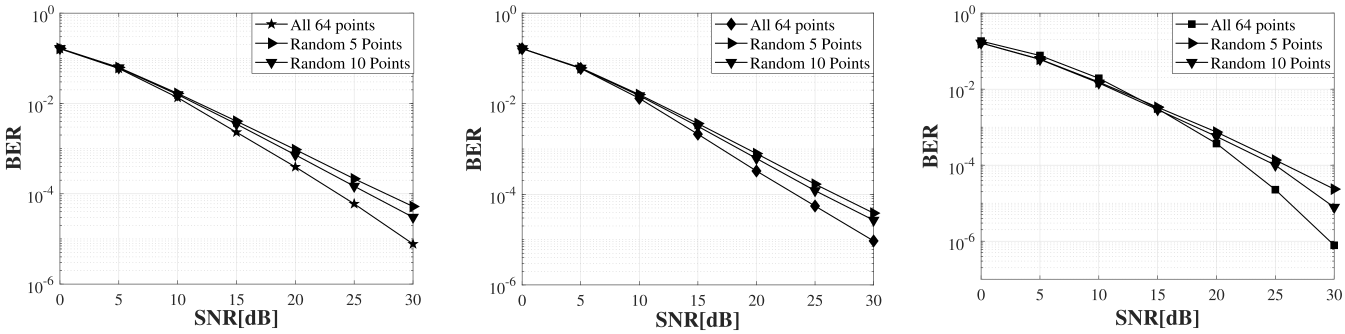

(a) The modified Alternating method (b) The modified Langrange Multiplier method (c) The modified PE-AltMin method

FIGURE 10. The three BER performances of each modified iterative methods in full-connected structure according to the different number of subcarriers.

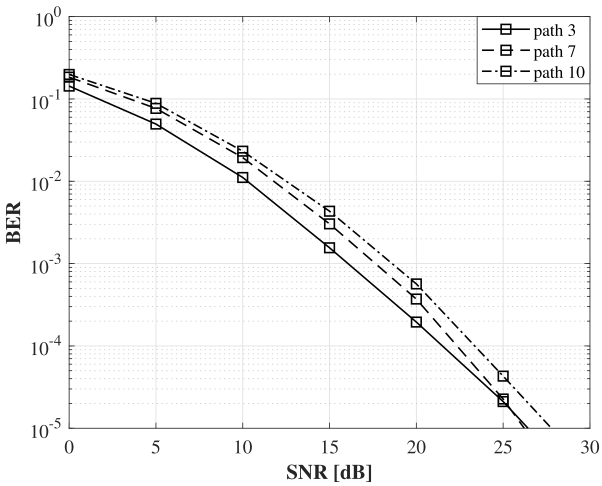

FIGURE 11. The BER performance of modified PE-AltMin method with different path in full-connected structure.

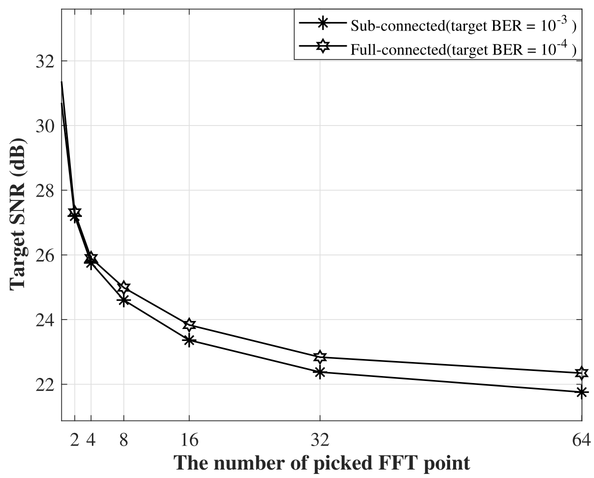

FIGURE 12. The required SNR performance of each target BER according to the number of picked FFT points.

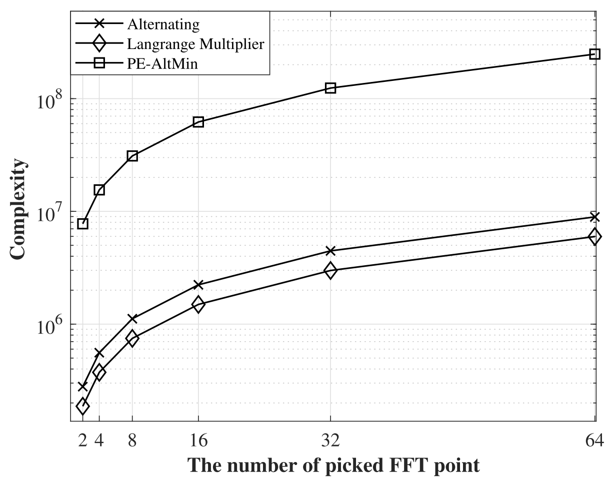

FIGURE 13. The complexity of three iterative methods according to the number of picked FFT points in full-connected structure.

in the iterative algorithm increases since the diversity gain is obtained. The proposed algorithm with iterative process shows similar tendency of performance despite the different updating methods. Also, the proposed algorithm can be simplified by the all numbers of antenna N.

Fig. 11 shows the BER performance of PE-AltMin method with iterating at all points of subcarrier in different path. The low performance is expected when the selectivity channel effect is increased. The Fig. 11 show that the performance is improved according to the path is decreased.

Fig. 12 shows the required SNR to achieve target BER in each structure when PE-AltMin method is used. The target BER in sub-connected is 10^{-3} and the target BER in full-connected is 10^{-4}. In both structures, when the more points are selected, the constant performance is reached more faster. We can check that the performance in Fig. 12 is obvious to get diversity gain refer to Fig. 5.

Fig. 13 shows the complexity for three iterative schemes at the full-connected structure. The complexity is considered by the number of calculation and deposition of matrixes and multiplied with the number of iterations. In this paper, the multiplying matrix, ZF and SVD are counted to calculate the computational complexity [33]. The total complexity can express as follows,

$$F_{tot} = F \cdot N_{iter} \cdot p, \tag{30}$$

where F is the complexity in each iterative scheme, N_{iter} is the average number of iteration in each subcarrier and p is the number of picked FFT point. The PE-AltMin has the highest complexity because of SVD calculation. Also, the simulation result shows the higher the number of picked FFT point, the complexity is increased.

VI. CONCLUSION

In this paper, the proposed algorithm with modified iterative schemes determines the analog precoding matrices by considering the power of hybrid precoding matrix. Both sub-connected and full-connected structures of hybrid beamforming system apply the modified Alternating, Langrange Multiplier and PE-AltMin iterative methods. The three iterative algorithms use at all subcarriers to make the candidates of analog precoding matrix. The final hybrid precoding matrix is selected by the smallest weight of analog and digital precoding matrices. Finally, the proposed algorithm improves the BER and the average sum rate of in wideband MIMO-OFDM hybrid beamforming system. For decreasing the complexity, the iterative algorithm uses at the random 5 and 10 points of subcarriers. The performances are improved as the number of used points in the iterative schemes increases. The diversity gain is obtained in the proposed algorithm according to the number of analog precoding matrices. Therefore, the proposed algorithm can be used in bad environment with the high reliable performance.

REFERENCES

[1] J. Zhang, E. Bjornson, M. Matthaiou, D. W. K. Ng, H. Yang, and D. J. Love, "Prospective multiple antenna technologies for beyond 5G," *IEEE J. Sel. Areas Commun.*, vol. 38, no. 8, pp. 1637–1660, Aug. 2020.

[2] E. Ali, "Beamforming techniques for massive MIMO systems in 5G: Overview, classification, and trends for future research," *Frontiers Inf. Technol. Electron.*, vol. 18, pp. 753–772, Jun. 2017.

[3] D. Zhu, B. Li, and P. Liang, "A novel hybrid beamforming algorithm with unified analog beamforming by subspace construction based on partial CSI for massive MIMO-OFDM systems," *IEEE Trans. Commun.*, vol. 65, no. 2, pp. 594–607, Feb. 2017.

[4] J.-H. Ro, W.-S. Lee, J.-G. Ha, and H.-K. Song, "An efficient precoding method for improved downlink massive MIMO system," *IEEE Access*, vol. 7, pp. 112318–112326, 2019.

[5] A. F. Molisch, V. V. Ratnam, S. Han, Z. Li, S. L. H. Nguyen, L. Li, and K. Haneda, "Hybrid beamforming for massive MIMO: A survey," *IEEE Commun. Mag.*, vol. 55, no. 9, pp. 134–141, Sep. 2017.

[6] O. E. Ayach, S. Rajagopal, S. Abu-Surra, Z. Pi, and R. W. Heath, Jr., "Spatially sparse precoding in millimeter wave MIMO systems," *IEEE Trans. Wireless Commun.*, vol. 13, no. 3, pp. 1499–1513, Mar. 2014.

[7] C. Kim, T. Kim, and J.-Y. Seol, "Multi-beam transmission diversity with hybrid beamforming for MIMO-OFDM systems," in *Proc. IEEE Globecom Workshops (GC Wkshps)*, Atlanta, GA, USA, Dec. 2013, pp. 61–65.

[8] X. Wei, Y. Jiang, Q. Liu, and X. Wang, "Calibration of phase shifter network for hybrid beamforming in mmWave massive MIMO systems," *IEEE Trans. Signal Process.*, vol. 68, pp. 2302–2315, 2020.

[9] F. Sohrabi and W. Yu, "Hybrid digital and analog beamforming design for large-scale MIMO systems," in *Proc. IEEE Int. Conf. Acoust., Speech Signal Process. (ICASSP)*, Brisbane, QLD, Australia, Apr. 2015, pp. 2929–2933.

[10] H. Li, M. Li, Q. Liu, and A. L. Swindlehurst, "Dynamic hybrid beamforming with low-resolution PSs for wideband mmWave MIMO-OFDM systems," *IEEE J. Sel. Areas Commun.*, vol. 38, no. 9, pp. 2168–2181, Sep. 2020.

[11] J. Mo, A. Alkhateeb, S. Abu-Surra, and R. W. Heath, Jr., "Hybrid architectures with few-bit ADC receivers: Achievable rates and energy-rate tradeoffs," *IEEE Trans. Wireless Commun.*, vol. 16, no. 4, pp. 2274–2287, Apr. 2017.

[12] J. Song, J. Choi, and D. J. Love, "Codebook design for hybrid beamforming in millimeter wave systems," in *Proc. IEEE Int. Conf. Commun. (ICC)*, London, U.K., Jun. 2015, pp. 1298–1303.

[13] A. Liu and V. K. N. Lau, "Impact of CSI knowledge on the codebook-based hybrid beamforming in massive MIMO," *IEEE Trans. Signal Process.*, vol. 64, no. 24, pp. 6545–6556, Dec. 2016.

[14] M. Li, Z. Wang, H. Li, Q. Liu, and L. Zhou, "A hardware-efficient hybrid beamforming solution for mmWave MIMO systems," *IEEE Wireless Commun.*, vol. 26, no. 1, pp. 137–143, Feb. 2019.

[15] H. Li, M. Li, and Q. Liu, "Hybrid beamforming with dynamic subarrays and low-resolution PSs for mmWave MU-MISO systems," *IEEE Trans. Commun.*, vol. 68, no. 1, pp. 602–614, Jan. 2020.

[16] B. Di, H. Zhang, L. Li, L. Song, Y. Li, and Z. Han, "Practical hybrid beamforming with finite-resolution phase shifters for reconfigurable intelligent surface based multi-user communications," *IEEE Trans. Veh. Technol.*, vol. 69, no. 4, pp. 4565–4570, Apr. 2020.

[17] F. Sohrabi and W. Yu, "Hybrid analog and digital beamforming for mmWave OFDM large-scale antenna arrays," *IEEE J. Sel. Areas Commun.*, vol. 35, no. 7, pp. 1432–1443, Jul. 2017.

[18] A. Alkhateeb and R. W. Heath, Jr., "Frequency selective hybrid precoding for limited feedback millimeter wave systems," *IEEE Trans. Commun.*, vol. 64, no. 5, p. 1801–1818, May 2016.

[19] L. Kong, S. Han, and C. Yang, "Wideband hybrid precoder for massive MIMO systems," in *Proc. GlobalSIP*, Orlando, FL, USA, Dec. 2015, pp. 305–309.

[20] Y. Sun, Z. Gao, H. Wang, B. Shim, G. Gui, G. Mao, and F. Adachi, "Principal component analysis based broadband hybrid precoding for millimeter-wave massive MIMO systems," *IEEE Trans. Wireless Commun.*, early access, Jun. 23, 2020, doi: 10.1109/TWC.2020.3002719.

[21] Z. Xu, S. Han, Z. Pan, and I. Chih-Lin, "Alternating beamforming methods for hybrid analog and digital MIMO transmission," in *Proc. IEEE Int. Conf. Commun. (ICC)*, London, U.K., Jun. 2015, pp. 1595–1600.

[22] X. Bai, F. Liu, and R. Du, "An alternating iterative hybrid beamforming method for millimeter wave large-scale antenna arrays," in *Proc. Prog. Electromagn. Res. Symp.*, Singapore, Nov. 2017, pp. 2769–2776.

[23] X. Yu, J.-C. Shen, J. Zhang, and K. B. Letaief, "Alternating minimization algorithms for hybrid precoding in millimeter wave MIMO systems," *IEEE J. Sel. Topics Signal Process.*, vol. 10, no. 3, pp. 485–500, Apr. 2016.

[24] B. Liu, W. Tan, H. Hu, and H. Zhu, "Hybrid beamforming for mmWave MIMO-OFDM system with beam squint," in *Proc. IEEE 29th Annu. Int. Symp. Pers., Indoor Mobile Radio Commun. (PIMRC)*, Bologna, Spain, Sep. 2018, pp. 1422–1426.

[25] F. Ademaj, M. Taranetz, and M. Rupp, "3GPP 3D MIMO channel model: A holistic implementation guideline for open source simulation tools," *EURASIP J. Wireless Commun. Netw.*, vol. 2016, no. 1, Feb. 2016.

[26] K.-N. Hsu, C.-H. Wang, Y.-Y. Lee, and Y.-H. Huang, "Low complexity hybrid beamforming and precoding for 2D planar antenna array mmWave systems," in *Proc. IEEE Workshop Signal Process. Syst. (SiPS)*, Hangzhou, China, Oct. 2015, pp. 1–6.

[27] R. Bohnke, D. Wubben, V. Kuhn, and K.-D. Kammeyer, "Reduced complexity MMSE detection for BLAST architectures," in *Proc. IEEE Global Telecommun. Conf.*, San Francisco, CA, USA, Dec. 2003, pp. 2258–2262.

[28] Y. Xiao, Y. Xiao, F. Yu, Y. Li, Y. Wang, and B. Fu, "Hybrid beamforming for large-scale MIMO-OFDM in frequency selective fading," in *Proc. Int. Symp. Netw., Comput. Commun. (ISNCC)*, Rome, Italy, Jun. 2018, pp. 1–4.

[29] L. Jiang and H. Jafarkhani, "Multi-user analog beamforming in millimeter wave MIMO systems based on path angle information," *IEEE Trans. Wireless Commun.*, vol. 18, no. 1, pp. 608–619, Jan. 2019.

[30] D. Brennan, "Linear diversity combining techniques," *Proc. IRE*, vol. 47, no. 6, pp. 1075–1102, Jun. 1959.

[31] A. Alkhateeb, O. El Ayach, G. Leus, and R. W. Heath, Jr., "Channel estimation and hybrid precoding for millimeter wave cellular systems," *IEEE J. Sel. Topics Signal Process.*, vol. 8, no. 5, pp. 831–846, Oct. 2014.

[32] J. P. Gonzalez-Coma, J. Rodriguez-Fernandez, N. Gonzalez-Prelcic, L. Castedo, and R. W. Heath, Jr., "Channel estimation and hybrid precoding for frequency selective multiuser mmWave MIMO systems," *IEEE J. Sel. Topics Signal Process.*, vol. 12, no. 2, pp. 353–367, May 2018.

[33] K. Zu and R. C. de Lamare, "Low-complexity lattice reduction-aided regularized block diagonalization for MU-MIMO systems," *IEEE Commun. Lett.*, vol. 16, no. 6, pp. 925–928, Jun. 2012.

SEULGI LEE was born in Seoul, South Korea. She received the B.S. degree in electronic information and communications engineering from Sejong University, Seoul, South Korea, in 2019, where she is currently pursuing the M.S. degree with the Department of Information and Communications Engineering. Her research interests include wireless communication systems design and multiple-input multiple-output signal processing.

WON-SEOK LEE received the B.S. and M.S. degrees in information and communication engineering, Sejong University, Seoul, South Korea, in 2016 and 2018, respectively, where he is currently pursuing the Ph.D. degree with the Department of Information and Communications Engineering. His research interests include signal processing for wireless communication systems and ambient RF communication systems.

JAE-HYUN RO was born in Seoul, South Korea, in 1989. He received the B.S. and M.S. degrees in information and communication engineering from Sejong University, Seoul, in 2015 and 2017, respectively, where he is currently pursuing the Ph.D. degree with the Department of Information and Communications Engineering. His research interests include digital communications and multiple-input multiple-output signal processing.

YOUNG-HWAN YOU received the B.S., M.S., and Ph.D. degrees in electronic engineering from Yonsei University, Seoul, South Korea, in 1993, 1995, and 1999, respectively. From 1999 to 2002, he was a Senior Researcher with the Wireless PAN Technology Project Office, Korea Electronics Technology Institute, Seongnam, South Korea. Since 2002, he has been a Professor with the Department of Computer Engineering, Sejong University, Seoul. His current research interests include wireless communication and signal processing with particular focus on wireless communications systems design.

HYOUNG-KYU SONG was born in Chungcheongbukdo, South Korea, in May 1967. He received the B.S., M.S., and Ph.D. degrees in electronic engineering from Yonsei University, Seoul, South Korea, in 1990, 1992, and 1996, respectively. From 1996 to 2000, he was a Managerial Engineer with Korea Electronics Technology Institute (KETI), South Korea. Since 2000, he has been a Professor with the Department of Information and Communications Engineering, Sejong University, Seoul. His research interests include digital and data communications and information theory and their applications with an emphasis on mobile communications.